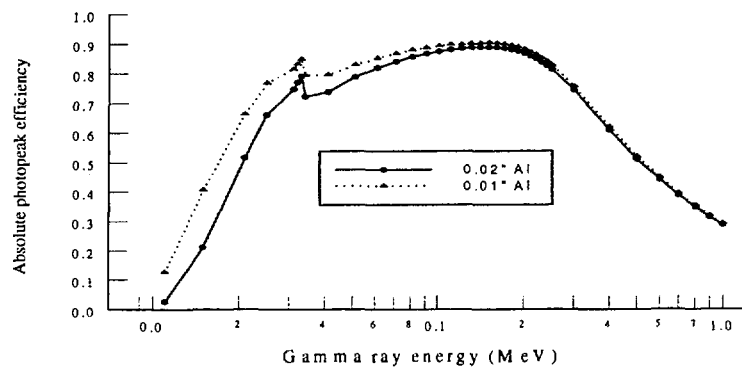




Anders Ringbom

# Development of detection techniques for the Swedish noble gas sampler



*L*

30 - 07

DEFENCE RESEARCH ESTABLISHMENT  
Division of NBC Defence  
SE-172 90 STOCKHOLM  
SWEDEN

FOA---98-00905-861---SE  
November 1998  
ISSN 1104-9154

Anders Ringbom

# **Development of detection techniques for the Swedish noble gas sampler**

Distribution: UD, Fö, HKV/PLANS, FMV, FRA, FHS, SSI, SKI, Skydds, ÖCB, SRV,  
Umeå Universitet

FOA: FOA GD, FOA Program, FOA Strategi, FOA Utland, FOA Avd 1-7

<b>Issuing organization</b> Defence Research Establishment Division of NBC Defence SE-172 90 STOCKHOLM SWEDEN	<b>Document ref. No., ISRN</b> FOA-R--98-00905-861--SE	
	<b>Date of issue</b> November 1998	<b>Project No.</b> E415, E417
	<b>Project name (abbrev. if necessary)</b> Detection and analysis	
<b>Author(s)</b>  Anders Ringbom	<b>Initiator or sponsoring organization</b> FOA, UD	
	<b>Project manager</b> Torbjörn Nylén	
	<b>Scientifically and technically responsible</b> Anders Ringbom	
<b>Document title</b> Development of detection techniques for the Swedish noble gas sampler		
<b>Abstract</b> A short review on the radioactive properties of noble gas isotopes relevant for monitoring of nuclear activities is given, together with a brief discussion of the existing systems for detection of radioactive noble gases. A $4\pi\beta\gamma$ detection system to be used in the automatic version of the Swedish noble gas sampling device is described. Monte Carlo (MCNP) calculations of the total gamma and beta efficiency for different detector designs have been performed, together with estimates of the resulting minimum detectable concentration (MDC). The estimated MDC values for detection of the $^{133}\text{gXe}$ 81 keV and the $^{135}\text{gXe}$ 250 keV gamma lines are around 0.3 mBq/m <sup>3</sup> in both cases. This is a factor of three lower than the detection limit required for a sampling station in the Comprehensive Nuclear-Test-Ban Treaty (CTBT) monitoring network. The possibility to modify the system to detect $^{85}\text{Kr}$ is also discussed.		
<b>Keywords</b> CTBT, radioxenon, beta-gamma coincidence, MCNP, $^{85}\text{Kr}$		
<b>Further bibliographic information</b>	<b>Language</b> English	
<b>ISSN</b> 1104-9154	<b>ISBN</b>	
	<b>Pages</b> p. 25	<b>Price</b> Acc. to pricelist
<b>Distributor (if not issuing organization)</b>		

<b>Dokumentets utgivare</b> Försvarets forskningsanstalt Avdelningen för NBC-skydd 172 90 STOCKHOLM	<b>Dokumentbeteckning, ISRN</b> FOA-R--98-00905-861--SE	
	<b>Dokumentets datum</b> November 1998	<b>Uppdragsnummer</b> E415, E417
	<b>Projektamn (ev förkortat)</b> Detektion och analys	
<b>Upphovsman(män)</b>  Anders Ringbom	<b>Uppdragsgivare</b> FOA, UD	
	<b>Projektansvarig</b> Torbjörn Nylén	
	<b>Fackansvarig</b> Anders Ringbom	
<b>Dokumentets titel i översättning</b> Utveckling av detektionsmetoder för det svenska systemet för insamling av ädelgaser		
<b>Sammanfattning</b> <p>Rapporten innehåller en kort översikt över de radioaktiva egenskaperna hos de ädelgasisotoper som är relevanta för monitorering av nukleära aktiviteter. Dessutom beskrivs kortfattat de system för ädelgasdetektion som finns idag.</p> <p>En <math>4\pi\beta\gamma</math>-detektor som skall användas i den automatiska versionen av det svenska systemet för ädelgasinsamling beskrivs. Monte Carlo (MCNP) beräkningar av den totala gamma- och betadetektionseffektiviteten hos olika detektorkonfigurationer har utförts, tillsammans med uppskattningar av den resulterande minsta detekterbara koncentrationen (MDC). Det uppskattade MDC-värdet för de dominerande gammasönderfallen från <math>^{133g}\text{Xe}</math> (81 keV) och <math>^{135g}\text{Xe}</math> (250 keV) är <math>0.3 \text{ mBq/m}^3</math> i båda fallen. Detta är en faktor tre lägre än den detektionsgräns som satts upp som krav för en insamlingsstation ingående i det nätverk som skall övervaka det fullständiga provstoppsavtalet (CTBT). Möjligheten att modifiera systemet för detektion av <math>^{85}\text{Kr}</math> diskuteras också i rapporten.</p>		
<b>Nyckelord</b> CTBT, radioxenon, beta-gamma koincidens, MCNP, $^{85}\text{Kr}$		
<b>Övriga bibliografiska uppgifter</b>	<b>Språk</b> Engelska	
<b>ISSN</b> 1104-9154	<b>ISBN</b>	
	<b>Omfång</b> s. 25	<b>Pris</b> Enligt prislista

**Distributör (om annan än ovan)**  
V.1.1

# Contents

<b>1</b>	<b>Introduction</b>	<b>5</b>
<b>2</b>	<b>Noble gas isotopes relevant for monitoring of nuclear activities</b>	<b>7</b>
<b>3</b>	<b>Existing systems for activity measurement of radioactive atmospheric noble gases</b>	<b>9</b>
<b>4</b>	<b>A detection system to be used in the Swedish noble gas sampler</b>	<b>12</b>
<b>5</b>	<b>Monte Carlo calculations of detector performance</b>	<b>15</b>
<b>6</b>	<b>Calculations of minimum detectable concentration (MDC)</b>	<b>18</b>
<b>7</b>	<b>Detection of <math>^{85}\text{Kr}</math></b>	<b>21</b>
<b>8</b>	<b>Summary and conclusions</b>	<b>23</b>
	<b>References</b>	<b>24</b>

# 1 Introduction

Airborne radioactive noble gas isotopes originate from several man made sources, including nuclear reactors, fuel reprocessing plants and nuclear explosions. About 20 identified radioactive isotopes of krypton and xenon, respectively, are formed in fission of heavy elements like uranium or plutonium.

In a nuclear power plant, most of these isotopes decay into non-gaseous elements before escaping from the fuel, but a few isotopes are sufficiently long-lived to cause an internal rod pressure which can cause cladding lift-off. Such a fuel-cladding failure can cause a release of radioactive noble gases into the coolant, and a subsequent release into the atmosphere. Noble gas releases from reactors are reported periodically [1]. The releases from individual reactors vary over a wide range (as an example the monthly release of  $^{133g}\text{Xe}$  from nuclear reactors in Sweden varied between 0.005 and 1.7 TBq in July 1998 [2]), and as a consequence the atmospheric concentration of radioactive noble gases also show large local variations. Annual mean values of the  $^{133}\text{Xe}$  concentration above 160 and below 4 mBq/kg of air has been reported (see [3] and references therein).

Less than 1% of the krypton produced in a reactor leaks through the fuel cladding during normal operation [4]. This is only a small amount compared to the  $^{85}\text{Kr}$  released from a reprocessing plant. A number of new, very large reprocessing plants devoted to civil uses, have recently, or will soon, come into operation [5]. Krypton is difficult to remove, and even the most modern facilities do not plan for  $^{85}\text{Kr}$  retention [6].

As is pointed out in ref. [5] stable noble gases are also formed during fission of heavy elements, and since the ratio of the stable isotopes are different compared to the natural isotopic abundance, measurement of the stable isotopes from the stack of a facility could serve as a verification technique. The isotopic abundances could give information on the burnup and type of fuel being processed. Detection of both stable and radioactive noble gases will be important tools when a future fissile material cut-off treaty (FMCT) is to be monitored.

An underground or underwater nuclear explosion is likely to vent the chemically inert noble gases into the atmosphere through the ground or the water. This makes detection of radioactive noble gases in general, and radioxenon in particular (see next section), an attractive tool for disclosing clandestine tests of nuclear weapons. To monitor compliance with the Comprehensive Nuclear-Test-Ban Treaty (CTBT) which now is signed by over 150 countries, an international network of stations is being set up [7], that will provide seismic, radionuclide, hydroacoustic and infrasound measurements. The map in fig. 1 shows the locations of the monitoring stations which together with the data center in Vienna constitutes the CTBT monitoring network. The radionuclide part of the network will consist of 80 stations worldwide, and in a first step 40 of these are scheduled to report measurements of radioxenon. Eventually all 80 stations might be equipped with radioxenon detection.

The Defence Research Establishment (FOA) in Sweden has been working with detection of radioactive xenon for many years [3], and a system for continuous sampling and analysis of  $^{133g}\text{Xe}$  has been in operation in Stockholm since 1990. A new automatic version of the system is planned to come into operation during 1999, and will together with a station in Argentina be the first station for xenon measurements

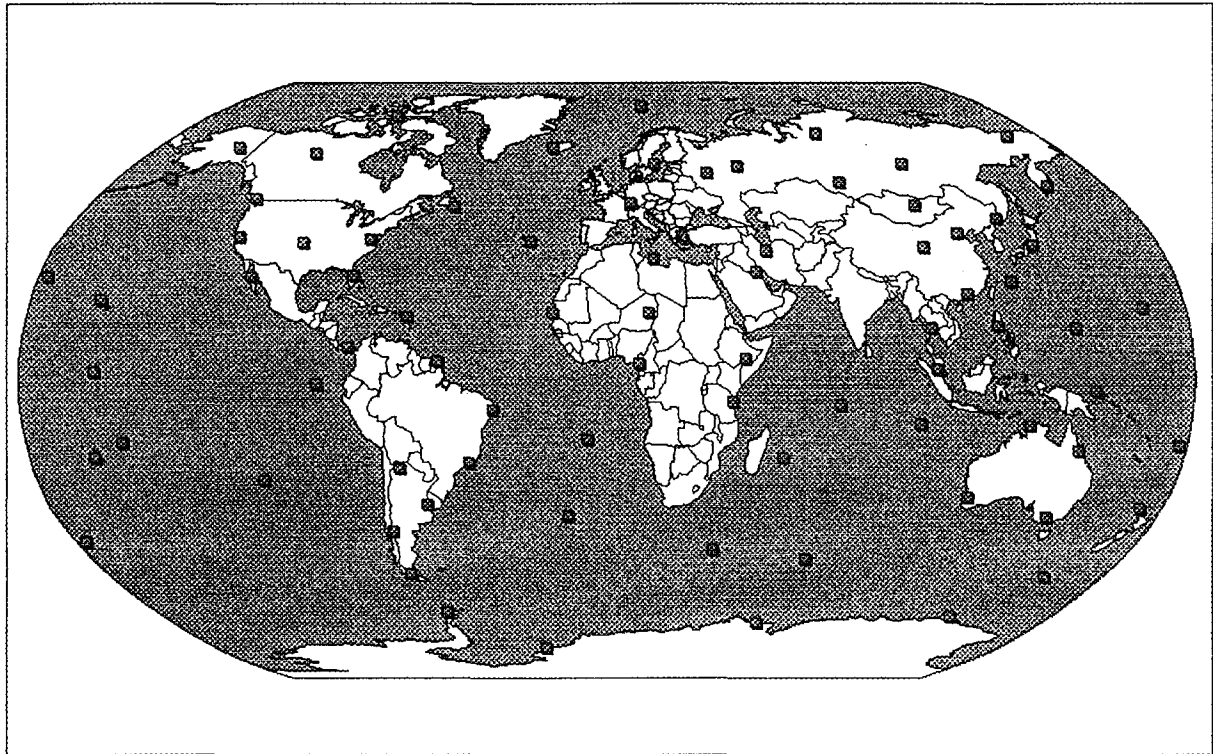


Figure 1: Map showing the locations of the radionuclide stations in the CTBT monitoring network.

included in the CTBT network.

The detector used to measure the activity of the collected xenon sample is for obvious reasons crucial for the quality of the measurement. In this report a short review of the current techniques for detection of radioactive noble gases is presented, together with a proposal for a detector to be used in the new version of the Swedish xenon sampler. Future possibilities for detection of  $^{85}\text{Kr}$  using this system are also discussed.

Section 2 contains a short review on the radioactive properties of the noble gas isotopes that are released from different man-made sources, and which of those that could be of interest for verification purposes. The existing systems for detection of atmospheric radioactive noble gases are briefly described in section 3, followed in section 4 by a discussion of some planned improvements of the detection methods used in the Swedish system. In particular a xenon detection scheme developed by Pacific Northwest National Laboratory (PNNL) is suggested to be modified and used also in the Swedish system. Monte Carlo calculations have been carried out in order to investigate the performance of such a detector. These are presented in section 5. An estimate of the minimum detectable concentration (MDC) that can be achieved using this detector can be found in section 6. A discussion of modifications necessary in order to facilitate measurements of  $^{85}\text{Kr}$  is given in section 7, while summary and conclusions are devoted to section 8.

## 2 Noble gas isotopes relevant for monitoring of nuclear activities

Krypton isotopes with mass numbers between 82 and 98 are produced in fission of  $^{235}\text{U}$  (with cumulative yields larger than  $1 \times 10^{-5} \%$  [8]). All of these isotopes have half lives shorter than 5 hours, with the exception of  $^{85}\text{Kr}$  which has a half-life of 10.73 years. Independent and cumulative fission yields for  $^{85}\text{Kr}$  for different fission types can be found in table 1. Since spent reactor fuel usually is stored for at least half a year before being reprocessed all krypton isotopes except  $^{85}\text{Kr}$  will have vanished when the irradiated fuel is being reprocessed. The continuous release of  $^{85}\text{Kr}$  from fuel reprocessing plants has resulted in a  $^{85}\text{Kr}$  contamination of the atmosphere that has increased steadily since the first plants came into operation [9]. The present average concentration in the northern hemisphere is about  $1 \text{ Bq/m}^3$ .

The decay scheme for this isotope is displayed in Fig. 2, showing that  $^{85}\text{Kr}$  is an almost pure beta-emitter. The endpoint energy for the beta particles is 687 keV. In activity studies the beta radiation is normally detected using gas proportional counters or plastic scintillators (see section 3).

In the case of xenon, the situation is a little bit different compared to krypton. Also here most isotopes produced in fission will decay within seconds, but a few isotopes will remain for several days, and are produced in such amounts that there is a relatively large probability that they can be detected at large distances from the position where they were emitted.

The xenon isotopes relevant for environmental sampling are  $^{131m}\text{Xe}$ ,  $^{133g}\text{Xe}$ ,  $^{133m}\text{Xe}$  and  $^{135g}\text{Xe}$ . The decay schemes for these isotopes are shown in Fig. 3, and

Isot.	Induc. spec.	$^{85}\text{Kr}$	$^{131m}\text{Xe}$	$^{133g}\text{Xe}$	$^{133m}\text{Xe}$	$^{135g}\text{Xe}$
$^{235}\text{U}$	Th. neutr. (i)	$2.55 \times 10^{-2}$	$3.48 \times 10^{-7}$	$6.66 \times 10^{-4}$	$1.89 \times 10^{-3}$	$7.85 \times 10^{-2}$
$^{235}\text{U}$	Th. neutr. (c)	$2.83 \times 10^{-1}$	$4.05 \times 10^{-2}$	6.70	$1.89 \times 10^{-1}$	6.54
$^{235}\text{U}$	Fiss. neutr. (i)	$3.09 \times 10^{-3}$	$2.41 \times 10^{-7}$	$1.46 \times 10^{-3}$	$4.23 \times 10^{-3}$	$1.20 \times 10^{-1}$
$^{235}\text{U}$	Fiss. neutr. (c)	$2.75 \times 10^{-1}$	$4.51 \times 10^{-2}$	6.72	$1.92 \times 10^{-1}$	6.60
$^{238}\text{U}$	Fiss. neutr. (i)	$1.99 \times 10^{-4}$	$3.16 \times 10^{-9}$	$4.18 \times 10^{-4}$	$1.22 \times 10^{-3}$	$1.11 \times 10^{-2}$
$^{238}\text{U}$	Fiss. neutr. (c)	$1.49 \times 10^{-1}$	$4.61 \times 10^{-2}$	6.76	$1.90 \times 10^{-1}$	6.97
$^{239}\text{Pu}$	Th. neutr. (i)	$1.00 \times 10^{-2}$	$3.00 \times 10^{-5}$	$9.45 \times 10^{-3}$	$3.38 \times 10^{-2}$	$3.14 \times 10^{-1}$
$^{239}\text{Pu}$	Th. neutr. (c)	$1.23 \times 10^{-1}$	$5.40 \times 10^{-2}$	7.02	$2.29 \times 10^{-1}$	7.61
$^{239}\text{Pu}$	Fiss. neutr. (i)	$9.47 \times 10^{-3}$	$2.67 \times 10^{-5}$	$1.58 \times 10^{-2}$	$4.65 \times 10^{-2}$	$6.14 \times 10^{-1}$
$^{239}\text{Pu}$	Fiss. neutr. (c)	$1.28 \times 10^{-1}$	$5.43 \times 10^{-2}$	6.97	$2.40 \times 10^{-1}$	7.54

Table 1: Independent (i) and cumulative (c) fission yields (%) for different fission types for the important krypton and xenon isotopes released into the atmosphere. Data are evaluated and recommended data obtained from ref. [8].

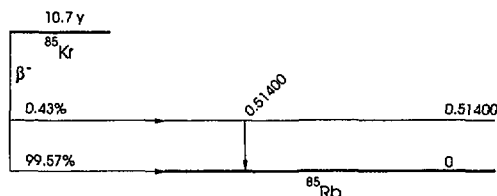


Figure 2: Simplified level scheme for  $^{85}\text{Kr}$  (energies in MeV).

fission yields can be found in table 1. Detection of the beta decay from a mixture of these xenon isotopes will result in a spectrum consisting of peaks originating from conversion electrons superimposed on a sum of several continuous beta distributions. The most intense conversion electron energies are found at 45 ( $^{133g}\text{Xe}$ ), 129 ( $^{131m}\text{Xe}$ ) and 199 ( $^{133m}\text{Xe}$ ) keV, respectively. In contrast to  $^{85}\text{Kr}$ , gamma spectroscopy can also be used to identify the different xenon isotopes. In addition to the X-ray peaks around 30 keV the dominating gamma peaks for  $^{133g}\text{Xe}$  and  $^{135g}\text{Xe}$  have energies of 81 and 250 keV, respectively. A summary [10] of the different decays of the relevant xenon isotopes sorted by energy is presented in table 2.

A calculation of the relative contribution of these four nuclides to the total xenon beta and electron activity as a function of time after fission can be found in ref. [10]. In these calculations it was assumed that the nuclides were produced by thermal fission of  $^{235}\text{U}$  and that there was no fractionation among the three mass chains. The result from this calculation is shown in Fig. 4. As can be seen in this figure the content of  $^{135g}\text{Xe}$  decreases exponentially and after about five days it has reached unmeasurable values. The  $^{133g}\text{Xe}$  activity will on the other hand remain at relatively large values for several weeks after the release, and the activity from  $^{131m}\text{Xe}$  will increase several days after fission and reaches a maximum after about 10 days, and remains at a high level for a couple of weeks. The  $^{133m}\text{Xe}$  activity will peak after about two days, and after that decrease exponentially.

When monitoring the xenon gas release from a subsurface nuclear detonation

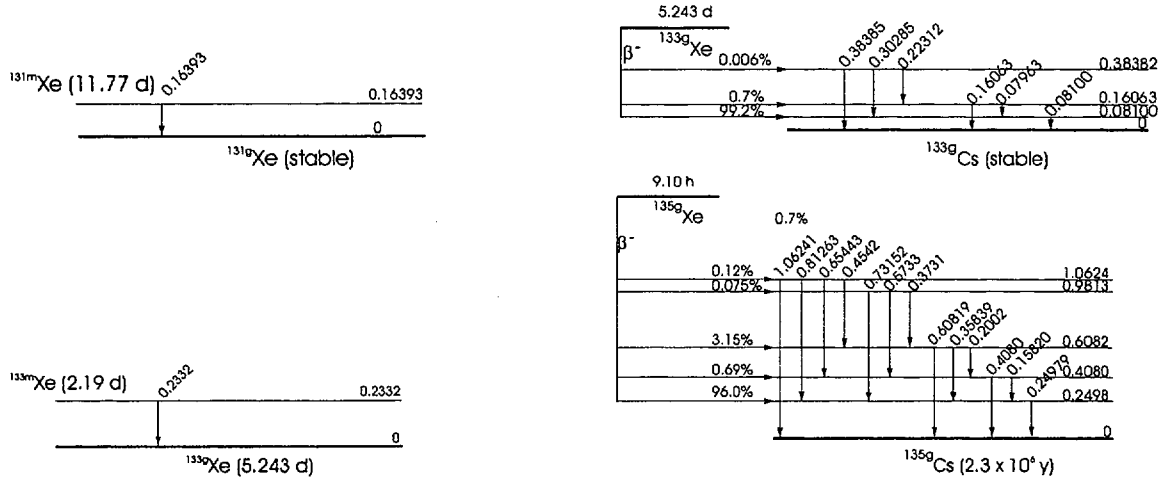


Figure 3: Simplified level schemes for xenon isotopes relevant for radioxenon measurements (energies in MeV).

the most important background is the release from nuclear power plants. According to calculations made in ref. [11] it will be possible to separate a power plant xenon release from a release originating in a nuclear explosion by inspecting the ratio between the different xenon isotopes. The ratio  $^{135g}\text{Xe}/^{133g}\text{Xe}$  is expected to be four orders of magnitudes larger for a subsurface nuclear explosion compared to a reactor release, and the value for  $^{133m}\text{Xe}/^{133g}\text{Xe}$  will differ by about a factor 100 between the two release types.

It is obviously very important that a detector system analysing xenon samples for the CTBT network has the capability to distinguish between  $^{135g}\text{Xe}$ ,  $^{131m}\text{Xe}$ ,  $^{133g}\text{Xe}$ , and  $^{133m}\text{Xe}$  in order to measure these isotopic ratios. This can be accomplished by a detector able to register both the beta and the gamma activity in coincidence, and preferably also having the capability to distinguish between the conversion electron energies discussed above.

### 3 Existing systems for activity measurement of radioactive atmospheric noble gases

Measurements of atmospheric  $^{85}\text{Kr}$  have been performed for many decades. See [12] for some early references. In this report the detection techniques used in a number of more recent measurement programmes will be briefly discussed. The programmes were originally presented in ref. [13].

A monitoring programme for radioactive noble gases is run by "Institut für Atmosphärische Radioaktivität" (IAR) located in Freiburg, Germany, where measurements of  $^{85}\text{Kr}$  have been performed since 1975 [9]. Cryogenic adsorption on charcoal at liquid nitrogen temperatures is used at different sites to collect krypton from air. The enriched samples are collected in aluminium bottles and shipped to

Decay energy (keV)	Decay intensity (%)	Decay type	Xenon isotope
29.46	15.4	Xe X-ray	131m
29.46	16.1	Xe X-ray	133m
29.46	3.8	Xe X-ray	135m
29.77	28.6	Xe X-ray	131m
29.77	29.8	Xe X-ray	133m
29.77	7.1	Xe X-ray	135m
30.63	14.1	Cs X-ray	133g
30.63	1.45	Cs X-ray	135g
30.97	26.2	Cs X-ray	133g
30.97	2.7	Cs X-ray	135g
33.60	10.2	Xe X-ray	131m
33.60	10.6	Xe X-ray	133m
33.60	2.5	Xe X-ray	135m
35.00	9.4	Cs X-ray	133g
35.00	0.97	Cs X-ray	135g
45.0	53.3	IC	133g
75.3	8.1	IC	133g
79.8	1.67	IC	133g
81	36.5	gamma	133g
129.4	61.2	IC	131m
158.5	28.6	IC	131m
162.8	6.5	IC	131m
164	2	gamma	131m
198.6	63.3	IC	131m
213.8	5.7	IC	135g
227.7	20.6	IC	133m
232.1	4.56	IC	133m
233	14	gamma	133m
249.8	90	gamma	135g
346 max	99.3	beta	133g
492.0	15.2	IC	135m
521.1	2.89	IC	135m
526.6	81	gamma	135m
608.2	2.9	gamma	135g
920 max	96.1	beta	135g

Table 2: Decay energies and types for certain radioactive xenon isotopes.

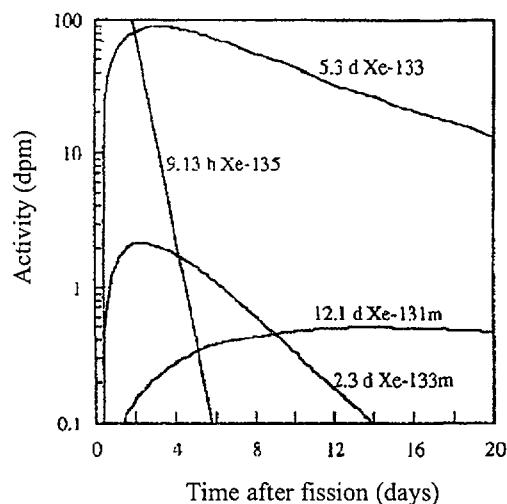


Figure 4: Activity of xenon isotopes in unfractionated mixed fission products from thermal neutron fission of  $^{235}\text{U}$  (figure taken from ref. [10]).

the laboratory in Freiburg for further purification and activity measurements. The gas is transferred to gas proportional counters using methane as a carrier gas, and the beta activity is determined using a gas proportional counter. The activity from radon that could remain in the gas is measured using alpha-counting. The stable krypton volume is determined by gas chromatography.

Measurements of  $^{85}\text{Kr}$  are also performed at the Moscow Engineering Physics Institute (MEPI) in Moscow. The counting method used here is different from the one used by the Freiburg group. The sample is transferred into a hollow plastic scintillator cylinder viewed by two PM-tubes in coincidence.

Plastic scintillators in a different configuration are used at the Laboratory of Geophysical Research, Vilnius, Lithuania. The detector consists of two plastic scintillator discs at the end of a cylindrical chamber. This method results in a rather low beta efficiency (5.5 %).

Another method is used by the U.S. Environmental Protection Agency, where the radioactive gas is transferred to a liquid scintillator cocktail and counted using PM-tubes. Here the efficiency should be considerably higher, on the other hand this method requires more manual work compared to the previous methods.

At Comenius University, Bratislava, Slovak Republic, the gas counting is performed using a proportional counter (efficiency = 71.5 %) operating in anticoincidence mode inside a plastic scintillator, which in turn is placed in a bulk shield.

Measurements of radioxenon are not as common and have not been performed for as many years as krypton measurements, and it is more difficult to find useful references on this subject. Work in this area have however been performed for many years in a few countries. Examples from USA, Germany, Russia and Sweden can be found in refs. [14], [15], [16], [17], and [3]. Collection and purification of the xenon gas is in most cases performed, just like in the case of krypton, by utilizing adsorption on charcoal and molecular sieves. In some cases noble gas concentrates

are collected from commercial air reduction plants and further purified before the activity is determined.

As can be seen in table 2 a xenon release originating from a nuclear power plant or a nuclear explosion results in a much more complex detection problem than the measurement of  $^{85}\text{Kr}$ , but on the other hand this can be used to obtain more accurate measurements using different coincidence techniques. The detection of the collected activity is performed by measuring the beta or gamma decay, or in some cases, a combination of both radiations. The group in Freiburg utilizes beta counting with proportional counters to detect the  $^{133g}\text{Xe}$  activity. Other groups reports detection of the gamma activity using a HPGe detector [15, 3]. In more recently developed techniques the beta and gamma radiation is recorded in coincidence using NaI detectors to detect the photons, and plastic scintillators [18] or surface barrier detectors [19] for beta or conversion electron detection.

## 4 A detection system to be used in the Swedish noble gas sampler

A system for continuous sampling and analysis of  $^{133}\text{Xe}$  has been in operation in the laboratory at Urvik, Stockholm, since September 1990. After a collection and concentration process the xenon gas sample is separated from radon utilizing a gas chromatograph. The xenon fraction is adsorbed on activated charcoal in a flat glass coil and analysed with respect to the 81 keV gamma radiation using a planar HPGe detector. The sampling capacity is currently about  $15\text{ m}^3/\text{day}$ , resulting in a detection limit of  $1.5 - 2\text{ mBq}/\text{m}^3$ .

A development of the sampling technique that aims towards a completely automatic system is now underway. The Swedish xenon sampler is at present semi-automatic, meaning that the samples have to be changed manually. Since the CTBT protocol requires 24 hour sampling a fully automatic system is necessary. A new sampling unit which can be run in automatic mode is therefore being developed [20]. This device is intended to be able to sample xenon close to room temperature, to reduce the dependence of freezers, and to be able to sample both xenon and krypton using a small freezer to cool the sampling air. In a first stage the system will measure xenon isotopes only, as required by CTBT. In a later stage, the system will be able to collect and purify  $^{85}\text{Kr}$  as well.

In order to improve the detection limit, and to make the process fully automatic, the procedure for the activity measurements of the collected samples has to be modified. The new detection system must provide automatic injection and removal of the gaseous xenon samples, it should perform gamma and beta detection with high efficiency and reproducibility and with low background. In addition, the system should be robust and relatively low-cost. Taking these facts into consideration, we have chosen to use a detector concept originally used by the group at PNNL [18, 21]. It is a beta-gamma coincidence system consisting of a number of cylindrical plastic scintillator cells surrounded by NaI crystals in a  $4\pi$  configuration. The xenon sample from the processing unit is transferred into the gas-cell trough a thin pipe (see Fig. 5). The beta particles from the xenon decay are detected in the 1 mm thick

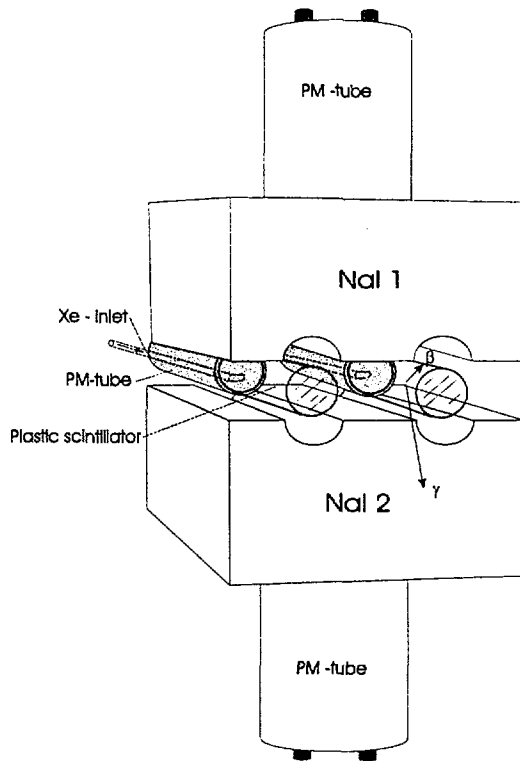


Figure 5: A beta-gamma system for detection of radioactive xenon. The PM-tubes at the front end of the scintillation cells are not shown.

plastic scintillator walls of the cell. Two PM-tubes, one at each end of the cylinder, are used to view the scintillator. In order to reduce the uncorrelated noise from the PM-tubes, the tubes are read out in coincidence, providing one beta signal only. This signal is used to gate the gamma-spectrum provided by the NaI crystals. In this way the signal-to-noise ratio is reduced by several orders of magnitudes. The background is further reduced by surrounding the entire system with a lead shielding. The PNNL-system consists of four scintillator cells and two NaI crystals, each crystal is viewed with two PM-tubes. The Swedish system will consist of fewer cells, probably two. The NaI crystals can be configured in several ways. One solution is to use two large crystals viewed with one PM-tube each (this solution is shown in Fig. 5). Another approach is to use smaller crystals with a cylindrical hole through the side of the crystal ("through-side well" configuration). In this construction the system would consist of two separate plastic-NaI combinations. One advantage with that configuration is that crosstalk between the scintillator cells is avoided.

The electronics needed to process the signals from the detector set-up is shown in Fig. 6. The figure shows the electronics needed for one scintillator cell in combination with two NaI crystals. The signals from the PM-tubes are divided into two branches. The logic branch provides the necessary gates to the ADCs, which are used to store the amplified analog pulses from the PM-tubes that comprises the other branch. This could be achieved using standard NIM or CAMAC modules read out using a PC equipped with a data acquisition software having two-parameter capability. If

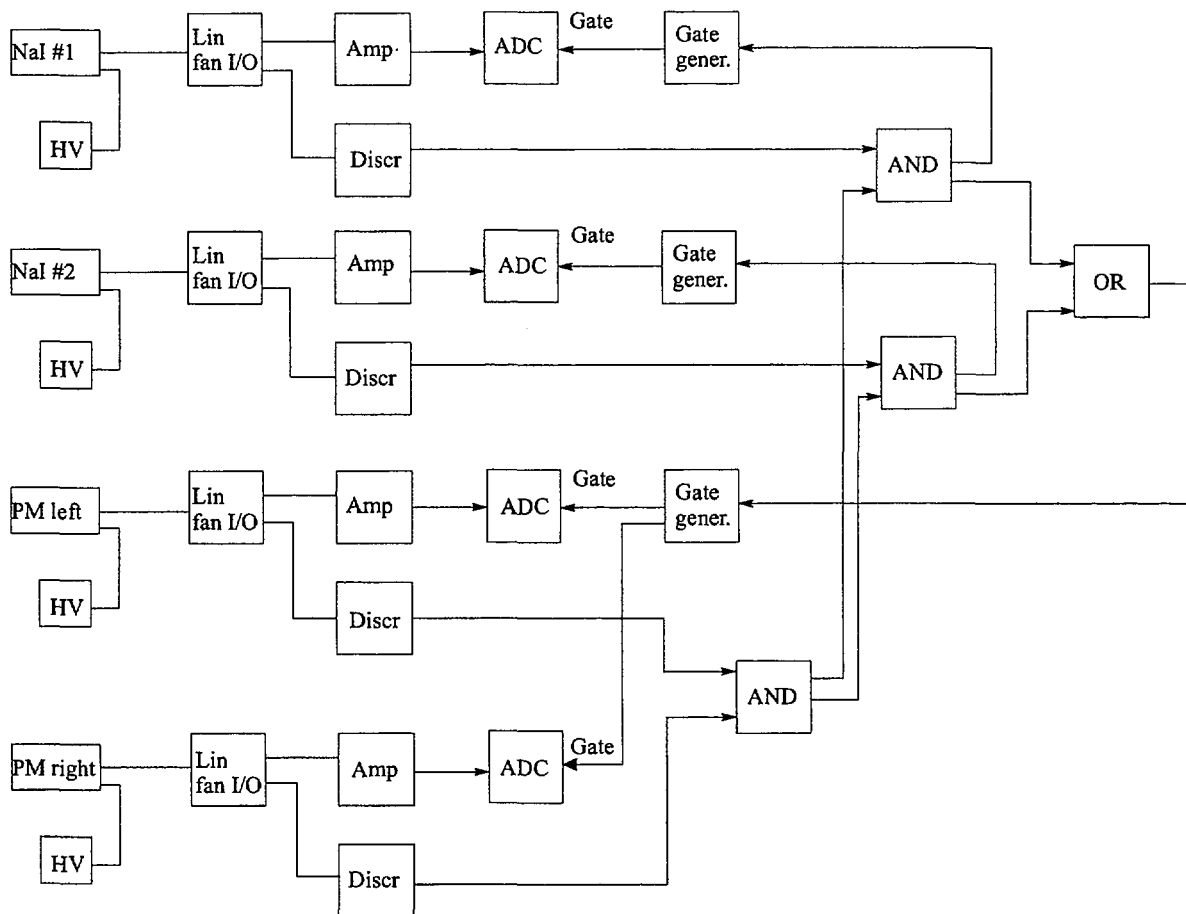


Figure 6: Schematic electronic scheme for the proposed beta-gamma coincidence system. This scheme is intended for a system consisting of two NaI crystals and one plastic scintillator cell.

the xenon sampler is to be duplicated in several copies for the CTBT network the electronics could be specially designed, built and placed into one module in order to reduce both size and cost.

The detector system described here is obviously just one out of several possible solutions. It is a compromise between capacity, cost and development time. In a later stage it would be very interesting to investigate what could be achieved with more sophisticated detectors, like HPGe for detection of gamma radiation and silicon surface barrier detectors to count the beta particles. The higher resolution that is possible to achieve using silicon detectors would improve the detection of conversion electrons, and thereby increase the possibility to distinguish between different isotopes, and also improve on the MDC. This parameter is of course also improved by the higher gamma energy resolution obtained by using HPGe detectors.

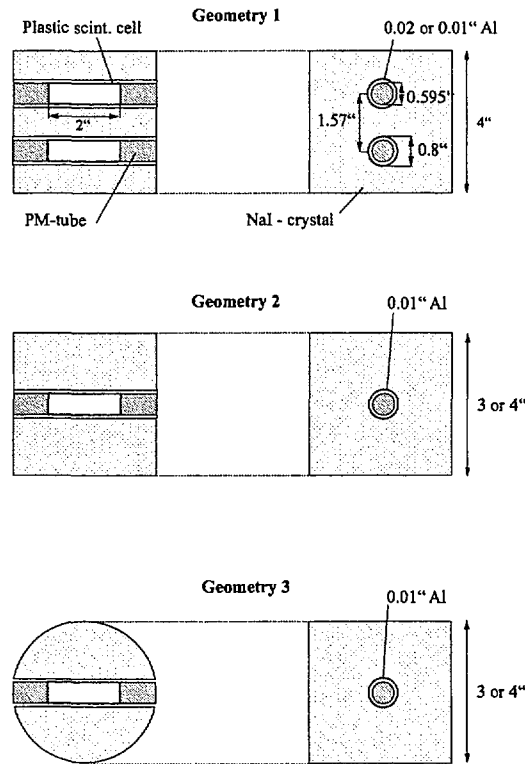


Figure 7: The three detector geometries studied in the MCNP calculations.

## 5 Monte Carlo calculations of detector performance

The proposed detector system should provide efficient detection of beta radiation with a maximum energy of about 1 MeV and of gamma rays with energies between 30 and 300 keV. In order to find appropriate size and geometry of the system, the response for both beta and gamma radiation have been studied with Monte Carlo calculations using the particle transport code MCNP [22]. Three different detector geometries were studied (see Fig. 7). One configuration (geometry 1) is close to the PNNL design, where several scintillator cells are surrounded by the same crystals. The two other geometries studied are based on one cell only, placed inside a NaI crystal having a through-side well configuration. The cylindrical version of the through-side well type NaI crystal in geometry 3 is available commercially as a standard configuration.

The following elements were included in the simulations:

i) One or two gas cells made out of BC404 plastic scintillator material. This material is based on polyvinyltoluene and has an atomic H/C ratio of 1.1 according to the manufacturer. It contains only traces of other elements which were not included in the calculations. The thickness of the cell walls was 1.2 mm.

ii) NaI crystal surrounded by a thin layer of aluminum. Different thicknesses of this layer was investigated. The layer should be made as thin as possible to allow efficient detection of low-energy gamma rays. On the other hand, it can not be made too thin since this would allow passage of beta-particles from the cell, resulting in

background.

iii) PM-tubes. These were modelled in a very simple way by homogenous aluminum cylinders. Test runs were also performed without these cylinders, resulting in a difference in photopeak efficiency of 5% for the lowest energies. For 250 keV photons the difference was less than 1 %.

In reality the plastic scintillator will be surrounded by some light shielding and reflecting materials. The small absorption caused by these materials was neglected in the calculations.

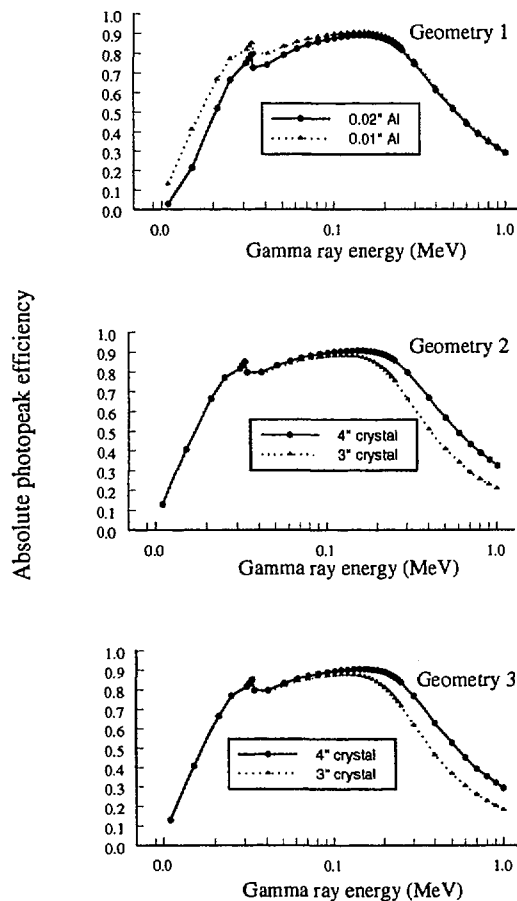


Figure 8: Calculated absolute photopeak efficiencies as a function of gamma ray energy for the three different geometries shown in Fig. 7.

The source particles (photons or electrons) were sampled homogeneously inside the plastic scintillator cylinder. In the case of photons a single energy was used in each run, and the energy deposited in the NaI crystal (and the cell walls) was tallied using the pulse height tally provided in MCNP. The code provides different ways to treat the photon induced reactions. In one mode, electrons are generated, but

are assumed to travel in the direction of the incident photon and are immediately annihilated (this is the "thick target bremsstrahlung" model). In this way the time consuming electron transport step is avoided. Another mode uses complete transport of the created electrons. Both modes were tested and it was found that the simpler treatment was sufficient in this case.

For each geometry the photopeak efficiency was calculated as a function of gamma ray energy. The results are displayed in Fig. 8. The variation of the light output with energy in NaI is not taken into account in the calculations. This variation is on the 10 % level below 400 keV [23]. The efficiency curves show only small differences for the different geometries. The absolute photopeak efficiency is 80 - 90 % in the energy range 30-300 keV. For smaller energies the efficiency decreases rapidly due to absorption of gamma rays in the scintillator cell and in the aluminium layer. The small peak around 30 keV is due to the K-shell absorption edge in iodine. For higher energies the efficiency decreases since many photons escape from the crystal before photoabsorption occurs. The effect of using a thicker aluminium layer enclosing the NaI crystal is illustrated in the uppermost panel of Fig. 8. Using 0.020" Al instead of 0.010" results in a decrease in efficiency of 10-15 % for the lowest relevant gamma energies. Furthermore, the efficiency for 300 keV gammas is reduced by the same amount if a 3" crystal is used instead of a 4" one, and the efficiency is only slightly lower using a cylindrical instead of a cubic NaI crystal.

The energy deposited by beta particles in the scintillator cell was also studied. The energy distribution of the source particles was assumed to be a continuous beta distribution. Calculated energy depositions in the plastic scintillator cell for beta distributions with decay energies corresponding to  $^{133g}\text{Xe}$  and  $^{135g}\text{Xe}$  are displayed in Fig. 9. Particles with the lowest energies are completely absorbed in the cell wall, in the case of  $^{133g}\text{Xe}$  resulting in a beta spectrum similar to the input spectrum. The increase and subsequent decrease in energy deposition starting at around 0.2 MeV for  $^{135g}\text{Xe}$  is due to particles passing through the beta detector, leaving only part of their energy in the scintillator material.

Having obtained the energy deposition in the cell it is possible to estimate the beta detection efficiency. The light output for electrons for a plastic scintillator material like polyvinyltoluene is linear above 125 keV deposited energy [24], and below this energy small nonlinearities are observed. Assuming a linear dependence also below 125 keV, and a discriminator threshold of 20 keV deposited electron energy (note that the coincidence requirement between the two PM-tubes viewing the scintillator cell will allow a lower threshold than would have been possible in a singles measurement), results in an efficiency of 94% for  $^{133}\text{Xe}$  and 99% for  $^{135}\text{Xe}$ . These numbers will in reality be somewhat reduced due to the gas inlet in the cell and the finite energy resolution which is not taken into account in the simulations. Assuming a total beta efficiency of 80% and combining this with the calculated gamma ray detection efficiency results in a total detector efficiency of about 65% in the relevant energy range. This value is used in the calculation of the MDC described in the next section.

In the case of  $^{135g}\text{Xe}$ , some electrons will reach the NaI crystal, resulting in false beta-gamma coincidences. This background was however found in the calculations to be very small in the region of the photopeak (around 1:1000). The problem will

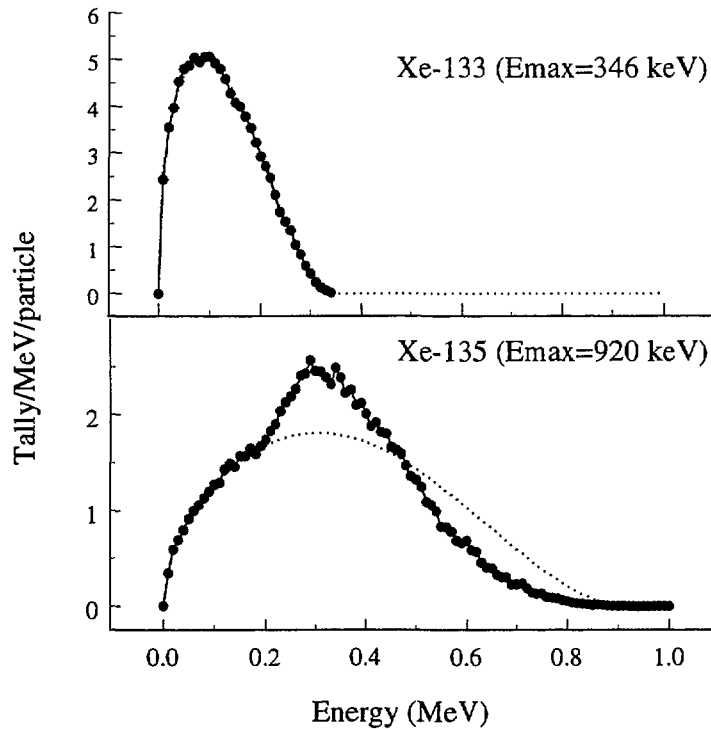


Figure 9: MCNP calculations of the energy deposition for beta particles in the plastic scintillator cell. The black points are calculated values, while the dotted lines shows the initial beta spectrum used in the calculations. In the case of  $^{133}\text{Xe}$  the two curves completely overlap since all beta particles are completely stopped in the scintillator.

not occur at all for  $^{133g}\text{Xe}$ , due to the lower beta energy for this isotope. One way to avoid this problem completely is to insert some additional material between the NaI detector and the beta detector.

## 6 Calculations of minimum detectable concentration (MDC)

The minimum detectable concentration (MDC) that can be expected for the FOA xenon autosampler using the proposed beta-gamma detector depends on a number of parameters. Since the detector system has not yet been constructed, the exact background conditions are not known, which means that it is difficult to calculate an accurate value of the MDC. However, using published data for the PNNL system together with some simple assumptions, an estimate of the expected detector performance can be made.

The integrated number of counts from a decaying isotope originally present in

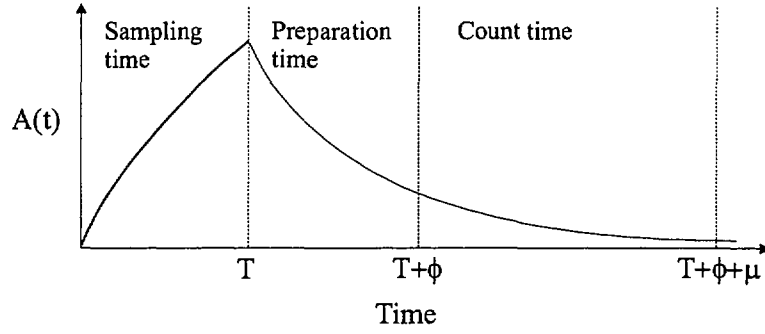


Figure 10: Definitions of time variables used in the calculations of the minimum detectable concentration.

the air sample, detected using beta-gamma coincidences and measured during a count time  $\mu$  is given by [25]

$$C(\phi, \mu) = \frac{\varepsilon_\gamma \varepsilon_\beta \gamma \beta \xi Q F}{\lambda^2} [1 - \exp(-\lambda T)] \exp(-\lambda \phi) [1 - \exp(-\lambda \mu)], \quad (1)$$

where  $T$  is the time of collection,  $\mu$  is the detector count time, and  $\phi$  is the preparation time for the xenon sampler (see Fig. 10). The air concentration for a given isotope is denoted by  $Q$ , and the volumetric flow rate by  $F$ . These two quantities are in general time-dependent, but are here assumed to be constant during the collection period, which is typically the case. The decay constant for the isotope under study is denoted by  $\lambda$ , the total detector efficiency for gamma and beta radiation by  $\varepsilon_\gamma$  and  $\varepsilon_\beta$ , the yield for the preparation process is represented by  $\xi$ , and  $\gamma$  and  $\beta$  are the abundances for the gamma and beta decays. The dead-time is neglected here, since the expected count rate is low. The qualitative picture of the corresponding activity as a function of time is sketched in Fig. 10.

Calculation of MDC is based on the concept of lower limit of detection (LD), which is the minimum number of source counts required for reliable detection. This number of counts obviously depends on the background rate, and often the following relation is used (see ref. [26] for further details):

$$LD = 2.71 + 4.65\sqrt{\mu_B}, \quad (2)$$

where  $\mu_B$  is the mean of the number of background counts in the region of interest in the gamma spectrum<sup>1</sup>. This expression is derived assuming a 5 % risk for type I (deciding that activity is present when it is not) or type II (failing to decide that it is present when it is) errors. The conversion from LD to the corresponding minimum detectable air concentration is then in this simplified case given by

$$MDC = \frac{LD}{\frac{\varepsilon_\gamma \varepsilon_\beta \gamma \beta \xi F}{\lambda^2} [1 - \exp(-\lambda T)] \exp(-\lambda \phi) [1 - \exp(-\lambda \mu)]}. \quad (3)$$

<sup>1</sup>This is the expression for a single channel. In reality the spectrum is recorded using several channels, and the expression then becomes:  $LD = 2.71 + 3.29\sqrt{\mu_B(1 + \frac{n}{2m})}$ , where the peak region covers  $n$  channels, and the background is determined using  $m$  channels on each side of the peak region [27]. Equation 2 is obtained by inserting  $n = 2m$  in this expression.

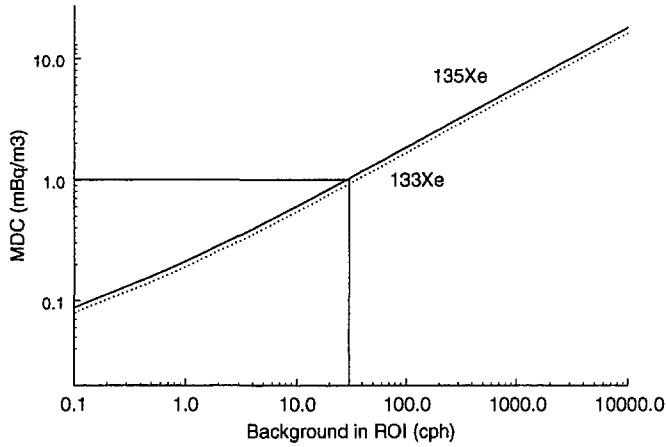


Figure 11: MDC as a function of the mean number of background counts in the region of the 81 and 250 keV photopeaks from gamma decay of  $^{133g}\text{Xe}$  and  $^{135g}\text{Xe}$ . A sampling and count time of 12 hours, and a preparation time of four hours are assumed. The other parameters used in the calculations are found in table 3. The CTBT limit of 1 mBq/m<sup>3</sup> is indicated in the figure.

Using the values of table 3 together with  $T = \mu = 12$  hours, and  $\phi = 4$  hours results in the following expressions for the MDC for detection of  $^{133g}\text{Xe}$  and  $^{135g}\text{Xe}$  using the 81 and 250 keV gamma lines, respectively, in coincidence with the corresponding beta radiation:

$$MDC_{133g} = 0.027 + 0.16\sqrt{\mu_B} \quad (4)$$

$$MDC_{135g} = 0.033 + 0.20\sqrt{\mu_B} \quad (5)$$

Equations 4 and 5 are plotted in fig. 11. The maximum MDC allowed by the CTBT organisation is 1 mBq/m<sup>3</sup>. As can be seen in the graph this demand is fulfilled if the background count rate does not exceed about 30 cph. The PNNL group reports a background count rate of 3.6 cph [21]. The same background conditions in the Swedish system would result in a MDC of 0.33 mBq/m<sup>3</sup>. The calculations thus indicates that even if the background conditions would be almost a factor of ten worse than in the American system, the CTBT demands would still be fulfilled. For comparison, the present Swedish xenon system has a MDC of 1.8 mBq/m<sup>3</sup> for the 81 keV peak, with a sampling time of 48 hours, and a preparation and counting time of 24 hours. The spectrum is recorded using a HPGe detector with an efficiency of 10% and a background in the region of interest of 70 cph. This illustrates the advantage of a coincident beta-gamma detector system compared to measuring gamma in singles mode.

In Fig. 12 the MDC is plotted as a function of collection and counting time, assuming a background count rate of 3 cph. As can be seen in the figure the MDC is a

	$^{133}\text{Xe}$ (81 keV)	$^{135}\text{Xe}$ (250 keV)
$F$ ( $\text{m}^3/\text{h}$ )	1.0	1.0
$\varepsilon_\gamma$ (%)	80	80
$\varepsilon_\beta$ (%)	80	80
$\gamma$ (%)	36.5	90
$\beta$ (%)	99	96.1
$t_{1/2}$ (h)	125.6	9.1

Table 3: Values of parameters used in the calculation of the MDC.

relatively constant function of the two times if both sampling and counting are performed for more than ten hours. The calculations predicts a MDC of  $0.34 \text{ mBq/m}^3$  for the 81 keV line in a  $^{133}\text{gXe}$  spectrum recorded for 12 hours. Increasing the count time to 24 hours results in a MDC of  $0.24 \text{ mBq/m}^3$ . Furthermore it can be noted that only two hours of counting is required to reach the CTBT limit of  $1 \text{ mBq/m}^3$  if the sample is collected for 12 hours.

To what extent would a shortening of the preparation time improve the MDC? Fig. 13 shows the MDC as a function of preparation time in the xenon sampler, assuming a sampling and counting time of 12 hours. As can be observed in the figure, lowering the preparation time will not affect the MDC very much in the case of  $^{133}\text{gXe}$ . This is because of the relatively long half life of this isotope compared to the preparation time. The sensitivity is larger for  $^{135}\text{gXe}$ , but a change in the preparation time from four to three hours would still only improve the MDC by about 7%.

A more efficient way of improving the sensitivity of the sampling device would be to increase the airflow ( $F$ ) through the system. It is possible that a small increase could be achieved by installing a stronger pump and using a different kind of charcoal in the adsorbers [20], but it is most probably too optimistical to claim that any significant improvement of  $F$  can be achieved using the present sampling technique.

In summary, the use of the beta-gamma coincidence technique together with good shielding and perhaps also some anti-coincidence arrangements, will reduce the MDC with an order of magnitude compared to the present system. It should be noted that an improved energy resolution of both the beta and the gamma detector would further decrease the background. This could be accomplished using silicon surface barrier- and germanium detectors. As already discussed, a higher beta-resolution would of course imply other advantages, like an improved capability to detect conversion electrons. Note however, that it has been shown that it is possible to identify the conversion electrons using the plastic scintillator cylinder by recording delayed coincidences between the beta particles that feed the 81 keV state in  $^{133}\text{Cs}$  and the conversion electron originating from deexcitation of that state [21].

## 7 Detection of $^{85}\text{Kr}$

Activity measurements of the pure beta-emitter  $^{85}\text{Kr}$  requires detection of beta particles in an almost background-free environment. As mentioned in section 3, existing methods use gas proportional counters or plastic scintillators to accomplish

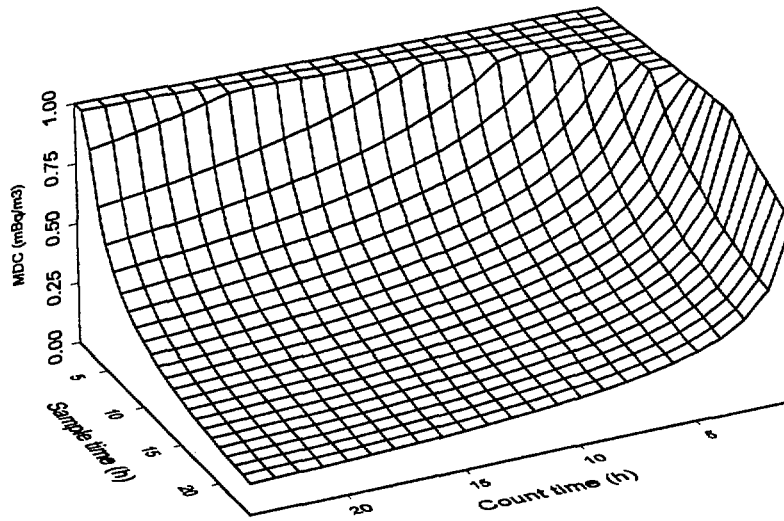


Figure 12: Calculation of minimum detectable concentration (MDC) for <sup>133</sup>Xe as a function of sampling and counting time, assuming the numbers given in table 3 and a preparation time of 4 hours.

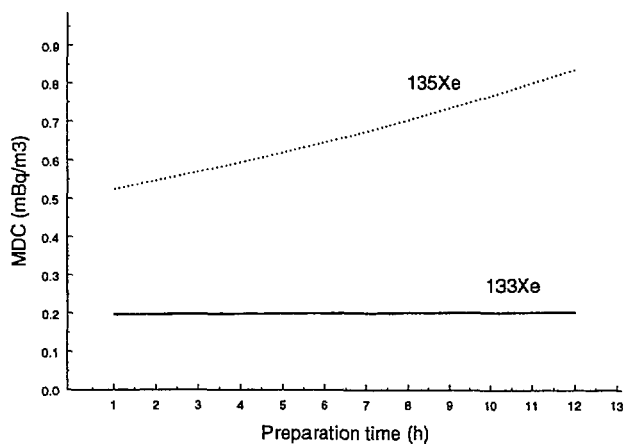


Figure 13: MDC for <sup>133</sup>Xe and <sup>135</sup>Xe as a function of preparation time in the xenon sampler, assuming a collection and counting time of 12 hours.

this. The background reduction is performed by applying passive shielding and/or using veto detectors, and sometimes the  $^{222}\text{Rn}$  content in the sample is checked using alpha-counting.

The FOA xenon autosampler can be modified to collect krypton as well. To measure the activity of the collected sample a gas proportional counter could be used, but it would of course be an advantage if the detector system suggested for xenon could be used also for this measurement. It is possible that this can be achieved, but there are some problems connected with this. Air contains  $1.14\text{ cm}^3$  natural krypton per  $\text{m}^3$ , and the corresponding number for xenon is  $0.086\text{ cm}^3$ . This means that the sample volume will be more than ten times larger for krypton compared to xenon if the same collection efficiency is assumed for the two gases, and it is probably not possible to use the suggested scintillator cells without measuring only a part of the krypton sample, which would cause an increase in the statistical error of the measurement. Another concern is the radon background, which has to be controlled. Although the separation between different noble gases in the sampler should be complete it is desirable that this could be monitored in some way using alpha detection.

In conclusion, it seems possible that measurement of both krypton and xenon using the same detector could be achieved, but practical tests are needed in order to clarify this question.

## 8 Summary and conclusions

An automatic version of the Swedish xenon sampler is planned to come into operation in 1999. It is suggested that the new version should be equipped with a  $4\pi\beta\gamma$  detector consisting of NaI crystals and plastic scintillator cells. Monte Carlo calculations have been performed to investigate the efficiency for different detector configurations. A standard  $4'' \times 4''$  crystal with through-side well configuration would give a total gamma ray detection efficiency of 80 % in the relevant energy range. The efficiency for detection of beta particles is in the same range. An estimate indicates a MDC of about  $0.3\text{ mBq/m}^3$  for a collection and counting time of 12 hours, respectively. It is possible that this value could be improved on by further development of the noble gas sampling method. The xenon sampler will fulfill the demands that is set up by the CTBT organisation, and can be used in the monitoring network of 80 radionuclide stations that is being set up around the world. The system can be further modified for detection of  $^{85}\text{Kr}$ , which might be of interest in a system monitoring a future fissile material cut-off treaty.

## References

- [1] "Sources and effects of ionizing radiation". UNSCEAR 1993 report to the General assembly.
- [2] Release data are obtained from the monthly release reports published by the different Nuclear Power stations in Sweden: Eva Fredriksson: "Forsmark - Utsläppsrapport juli 1998 (FQ-Rapport Nr 98/064)", Catarina Goldstrand: "Barsebäck, Månadsrapport för juli 1998 (Nr P2-9809-73)", Louise Klingstedt Pettersson: "Oskarshamnsverken - Månadsrapport för juli 1998 (Nr 98-11635)", and Lisbeth Helgesson: "Ringhals Månadsrapport för juli 1998 (0656/98)".
- [3] Brita Bernström and Lars-Erik De Geer. *FOA Report*, C 20515-A1, (1983).
- [4] National Council on Radiation Protection and Measurements, NCRP Report No. 44 (July 1975).
- [5] C. W. Nakhleh, W. D. Stanbro, L. N. Hand, R. T. Perry Jr., W. B. Wilson, and B. L. Fearey. *Science & Global Security*, **6**, 357, (1997).
- [6] "Plutonium - Deadly Gold of the Nuclear Age", International Physicians for the Prevention of Nuclear War and The Institute for Energy and Environmental Research, International Physician Press, Cambridge, Massachusetts, 1992.
- [7] <http://www.ctbto.org/>.
- [8] T. R. England and B. F. Rider. *Los Alamos National Laboratory Report LAUR-94-3106*, (October 1994). See also <http://t2.lanl.gov/publications/yields>.
- [9] W. Weiss, H. Sartorius and H. Stockburger. "Global distribution of atmospheric Kr-85" in *"Isotopes of Noble Gases as Tracers in Environmental Studies"* (Vienna: IAEA, 1992), pp 29-62.
- [10] W. R. Schell, M. J. Tobin, D. J. Marsan, C. W. Schell, J. Vives-Batlle, and S. R. Yoon. *Nucl. Instr. Meth. Phys. Res.*, **A385**, 277, (1997).
- [11] R. W. Perkins and L. A. Casey. *DOE/RL-96-51*, (June 1996).
- [12] I. Schröder, K. O. Münnich, and D. H. Ehhalt. *Nature*, **233**, 614, (1971).
- [13] "Report of an Expert Consultation on Kr-85 and Rn-222 Measurements, Effects and Applications". World Meteorological Organization, Global Atmosphere Watch, Environmental Pollution Monitoring and Research Programme Report Series, **109**, 1995.
- [14] C. O. Kunz and C. J. Paperiello. *Science*, **192**, 1235, (1976).
- [15] T. W. Bowyer, K. H. Abel, W. K. Hensley, M. E. Panisko, and R. W. Perkins. *J. Environ. Radioactivity*, **37**, 143, (1997).
- [16] von H. Stockburger, H. Sartorius, and A. Sittkus. *Z. Naturforschung*, **32A**, 1249, (1977).

- [17] Yu. V. Dubasov and Yu. S. Popov. In *Proceedings of the International Symposium "Monitoring and Discrimination of Underground Nuclear Explosions and Earthquakes"*, pages 163–172, November 1997.
- [18] P. L. Reeder and T. W. Bowyer. *Nucl. Instr. Meth. Phys. Res.*, **A408**, 582, (1998).
- [19] G. P. Lamaze. *Nucl. Instr. Meth. Phys. Res.*, **A385**, 285, (1997).
- [20] Tuula Larsson, private communication.
- [21] P. L. Reeder and T. W. Bowyer. *Nucl. Instr. Meth. Phys. Res.*, **A408**, 573, (1998).
- [22] J. F. Briesmeister. *Los Alamos Natl. Lab. report*, LA-12625-M, (1997).
- [23] D. Aitken, B. L. Leron, G. Yenicay, and H. R. Zulliger. *Trans. Nucl. Science*, **NS-14**, 468, (1967).
- [24] D. L. Smith, R. G. Polk, and T. G. Miller. *Nucl. Instr. Meth.*, **64**, 157, (1968).
- [25] W. C. Evans. *PSR Technical Note 1079*, (1995).
- [26] L. A. Currie. *Analytical Chemistry*, **40**, 586, (1968).
- [27] G. Gilmore and J. Hemingway. *"Practical GammaRay Spectrometry"*. John Wiley & Sons, (1996).